Titel/Title: Prevention of wheel clogging in creep feed grinding by efficient tool cleaning

Autor*innen/Author(s): C. Heinzel, G. Antsupov

Veröffentlichungsversion/Published version: Postprint

Publikationsform/Type of publication: Artikel/Aufsatz

Empfohlene Zitierung/Recommended citation:

C. Heinzel, G. Antsupov: Prevention of wheel clogging in creep feed grinding by efficient tool cleaning. CIRP Annals, Volume 61, Issue 1, 2012, Pages 323-326, ISSN 0007-8506, https://doi.org/10.1016/j.cirp.2012.03.056. (https://www.sciencedirect.com/science/article/pii/S0007850612000583)

Verfügbar unter/Available at:
(wenn vorhanden, bitte den DOI angeben/please provide the DOI if available)

https://doi.org/10.1016/j.cirp.2012.03.056

Zusätzliche Informationen/Additional information:

Prevention of wheel clogging in creep feed grinding by efficient tool cleaning

C. Heinzel (2), G. Antsupov
University of Bremen, Department of Manufacturing Processes, Badgasteiner Str. 1, 28359 Bremen, Germany

This paper is dealing with the identification of efficient cleaning nozzle configuration to prevent the wheel from loading in creep feed grinding. The properties of different cleaning nozzles types were analyzed in terms of jet velocity and jet impact on the wheel surface using high speed imaging and pressure sensitive sheets. In grinding experiments the cleaning efficiency of each nozzle configuration was evaluated by optical measurement of wheel clogging inside the machine tool. With this newly developed procedure of tool cleaning optimization a significant reduction of grinding forces (up to 30%) and of the tool wear (up to 20%) was achieved.

1 Introduction and state of the art

1.1 Clogging of grinding tools

Creep feed grinding is characterized by a high achievable process performance and a high achievable workpiece quality. Due to the high depth of cut (up to 50 mm) a wide contact length between the workpiece and the grinding wheel is obtained. This is disadvantageous for the coolant supply to the workpiece as well as for the chip transport from grinding zone and leads often to clogging of the grinding wheel. In creep feed grinding of ductile materials, chip nests in the tools' pore space and so-called welded clogging on the grinding grains usually arise. This impairs the cutting ability of the grinding tool, leading to increased grinding forces and high temperatures in the contact zone. Therefore, the risk of workpiece damage is drastically increased [1, 2, 3].

Wheel clogging can be reduced by optimizing the process parameters, the coolant supply, the tool design and the tool conditioning [1, 4]. High-pressure coolant supply can achieve not only highly effective cooling and lubrication but may also be used to prevent wheel clogging [5]. Optimizing of the coolant supply (nozzle design, nozzle position) can result in effective cooling lubrication in grinding operations, even at low pressure or low flow rate [6, 7]. However, the cleaning effect of the low-pressure coolant jet is not always strong enough to remove wheel clogging. In this case, it is up to now necessary to perform in-process or post-process wheel conditioning with dressing tools and/or sharpening blocks [4]. The Laser beam and the abrasive waterjet can also be used for this purpose [8, 9].

In industrial high-performance grinding processes, additional nozzles are often used for in-process tool-cleaning and thus for prevention of wheel clogging. It was shown that wheel cleaning with coolant jet leads to significant improvements in the grinding process with regard to the grinding forces, tool life time and workpiece quality [2, 5]. It should be noted that often a high pump pressure up to 100 bar and/or a high flow rate up to 400 l/min are required to effectively prevent wheel clogging [2, 5, 10]. However, for industrial application low pressures and flow rates would be favourable. But the selection of appropriate parameters for efficient grinding wheel cleaning by means of additional cleaning nozzles is still a difficult task which is due to a lack of understanding of the cleaning effect itself and its monitoring.

The flow properties of the cleaning jet and its interaction with the wheel surface determine the achievable cleaning performance and thus the tool condition. Therefore in the following, the basic characteristics of jet flow and liquid-solid impact are described, which are of crucial importance for design and development of high-efficient cleaning processes for grinding tools.

1.2 Basic characteristics of liquid-solid impact

Fig. 1 shows the structure of a high-speed (v_j > 50 m/s) waterjet which is divided into three zones. In the jet core zone, laminar flow with constant jet velocity occurs. The collision of the laminar waterjet with a solid generates the stagnation pressure p_s on the target surface which can be calculated according to a simplified Bernoulli equation (Eq. 1) [11],

$$p_s = \frac{1}{2} \cdot \rho_f \cdot v_j^2 \qquad (1)$$

where ρ_f and v_j are the fluid density and the jet velocity.

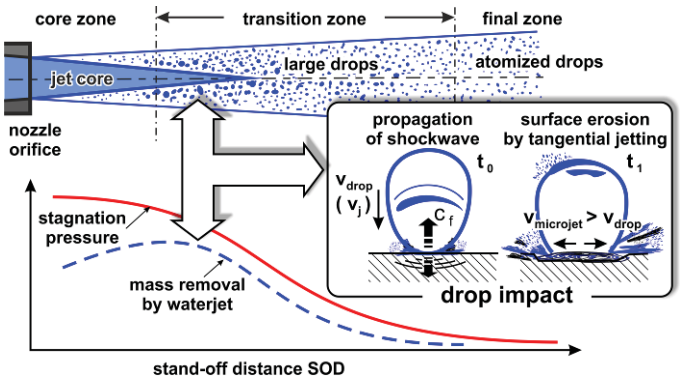

Figure 1. Structure of high-speed waterjet, drop impact, stagnation pressure and mass removal by waterjet depending on stand-off distance (after [12, 13])

The interaction of the water jet with air and the resulting turbulences lead to formation of large drops and drop collectives in the jet transition zone. The large drops give the jet a high dynamics, which, at a certain nozzle distance from the target surface (stand-off distance *SOD* in Fig. 1) can lead to an increased cleaning effect of the waterjet. During the drop collision with a solid surface, a shockwave within the drop can arise, due to the water compressibility. This shockwave propagates at the speed of sound (c_f ≈ 1,500 m/s for water) and leads to the so-called water-hammer pressure p_{wh} on the target surface. The load exerted on the surface by the shockwave lasts for a few milliseconds and can be estimated using the Cook equation (Eq. 2) [13, 14].

$$p_{wh} = \rho_f \cdot c_f \cdot v_j \qquad (2)$$

The initial shock in the drop-solid contact zone causes a tangential flow with microjets across the target surface (Fig. 1). The microjets have a velocity up to ten times higher than that of the initial drop and can exert a strong shear stress on the surface, which can lead to surface damages by erosion [13, 14]. However, the impact of liquid-jet on the solid surface is difficult to investigate due to the extremely short duration time of the shock propagation. The origin of resulting surface damage remains therefore not fully understood [15]. In most cases, the cleaning effect of the waterjet can only be determined experimentally.

2 Research approach

As part of this research work, correlations between the flow properties of cleaning nozzles and their cleaning performance in grinding experiments were investigated. The properties of different cleaning nozzle types were analyzed regarding jet velocity and jet impact on the wheel surface. In grinding experiments, the cleaning performance of each nozzle type was evaluated by measurement of wheel clogging and grinding forces.

3 Investigation of nozzle flow properties

3.1 Nozzle characteristics

Three types of cleaning nozzles with comparable orifice areas were investigated. The nozzle specifications are listed in Tab. 1. The mean jet velocity at a stand-off distance *SOD* of 30 to 100 mm was measured by high-speed photography (Fig. 2). The static pressure in the nozzle $p_{n.s}$ was varied in range from 10 to 40 bar.

Table 1. Specifications of the investigated cleaning nozzles

Nozzle type	Flat fan		Needle	Rotor
Nozzle designation	F71	F42	N71	R42
Orifice area, mm^2	7.1	4.2	7.1	4.2
Jet opening angle, °	20	20	-	20
Number of jet revolutions, s^{-1}	-	-	-	100 (on 20 bar)

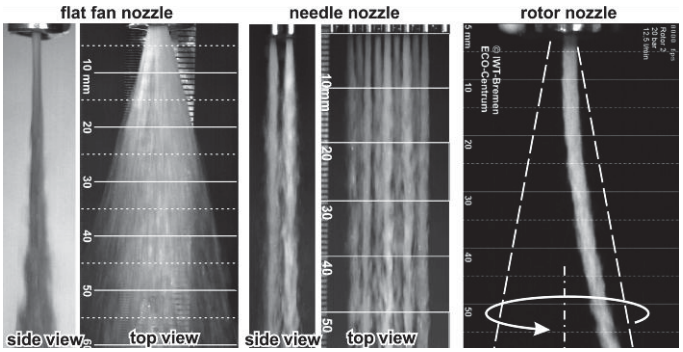

Figure 2. High-speed photographs of the investigated cleaning jets

Despite the comparable nozzle orifice areas, differences were detected in both, the jet velocity v_j and in the volumetric flow rate Q_f (Fig. 3). These differences are effects of the internal nozzle design and flow conditions within the respective nozzle. The jet velocities of the flat fan nozzles F71 and F42 are around 80% and 25% higher than those of the needle nozzle N71 and the rotor nozzle R42. Reducing the nozzle orifice area from 7.1 mm^2 to 4.2 mm^2 in flat fan nozzles leads to a decrease in jet velocity by around 25% and in flow rate by around 48%.

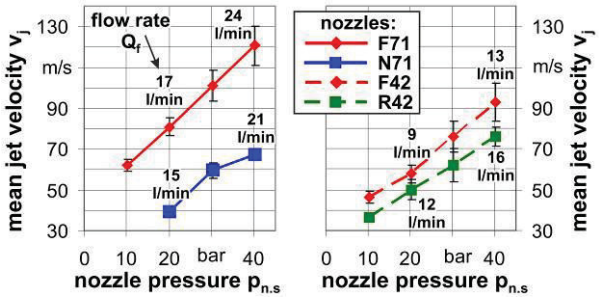

Figure 3. Jet velocity and flow rate in depending on nozzle design and internal nozzle pressure

3.2 Jet impact pressure

For measurement of the jet impact pressure, PRESCALE® pressure sensitive sheets (PSS) were used (Fig. 4). These sheets are coated with microcapsules of different wall thicknesses and sizes. When pressure is applied, the microcapsules burst and release the reagent liquid, which causes a discoloration of the sheet. Increasing the pressure leads to intensified discoloration of the PSS. The sheet is then scanned and the color intensity distribution of the scanned sheet is converted into a pressure distribution using software from the PSS manufacturer.

The microcapsules of PSS are very small - a few micrometers in diameter. It is therefore conceivable that the jet impact pressure can be measured on the micro level by this means. The measured result can be interpreted as the superimposed effect of the jet stagnation pressure, the water-hammer pressure and the shear stress by tangential flow.

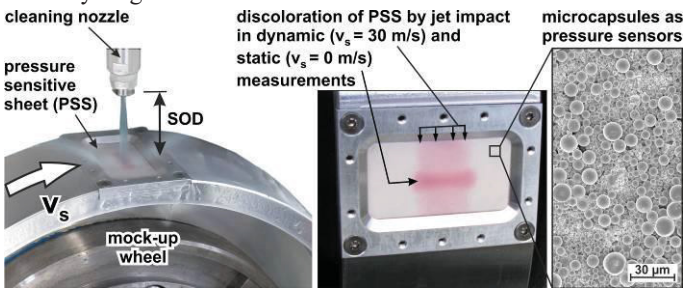

Figure 4. Measurement of jet impact pressure

PSS were applied to a mock-up wheel (Fig. 4). Static measurements of the jet impact pressure were carried out on a fixed wheel, while dynamic pressure measurements were conducted on a rotating wheel (v_s = 30 - 80 m/s). Fig. 5 shows the distribution of the jet impact pressure, which was recorded in static pressure measurements with nozzles F71, N71 and R42. At a nozzle distance of *SOD* = 50 mm and a static pressure of $p_{n.s}$ = 20 bar, the maximum jet impact pressure $p_{i.max}$ is around 50 MPa for the flat fan nozzle, and around 10 MPa for the needle and rotor nozzles. The dependence of the maximum impact pressure $p_{i.max}$ on the stand-off distance *SOD* is shown in Fig. 6. In static measurements at SOD = 30 - 100 mm, the nozzles F42 and F71 have an up to 80% higher jet impact pressure $p_{i.max}$ compared to the nozzles R42 and N71 (Fig. 6, left). In agreement with the theory (Eq. 1 and 2), these results show that the measured impact pressure p_i is mainly determined by the jet velocity v_j and thus by the nozzle design.

In dynamic measurements with nozzle F71, a decrease from 10% up to 70% in the jet impact pressure was observed when increasing wheel speed v_s from 30 m/s to 80 m/s (Fig. 6, right). It is assumed that the reason for this observation is the shortening of jet exposure time as well as the increasing of the influence of the so-called air barrier on the wheel surface at higher wheel speed.

The maxima of impact pressure were observed at a stand-off distance of 35 mm for nozzle F42 and of 50 mm for nozzle F71. With the nozzles R42 and N71, an increase in the jet impact pressure was observed at stand-off distances from 35 up to 85 mm. It should be noted that the 'optimal' stand-off distance with the maximum pressure remains constant when wheel speed v_s (30 - 80 m/s) and/or static pressure in the nozzle $p_{n.s}$ (20 – 40 bar) is varied. The effect of stand-off distance can be explained by analyzing of the jet structure. High-speed photographs (Fig. 2) show turbulence in the jet, beginning from SOD = 10 – 15 mm for the needle nozzle and SOD = 30 – 40 mm for the rotor nozzle. Formation of numerous drop collectives was observed at SOD = 25 and 40 mm for the flat fan nozzles F42 and F71. These structural disturbances in the jet can lead to a high-frequently drop impact and thus to higher shear stress on the target surface. Further increasing the stand-off distance, especially with flat fan nozzles, leads to distribution of the jet energy and the flowing liquid mass across a larger area. The increasing turbulences cause a decrease in jet velocity and support the formation of smaller drops in the jet. This all leads ultimately to a decrease in jet impact pressure.

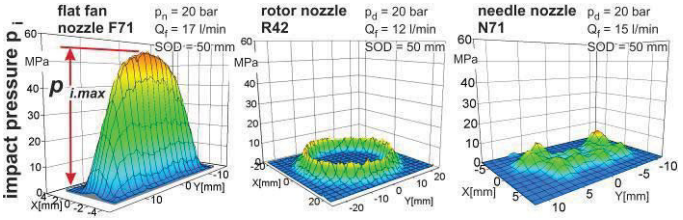

Figure 5. Distribution of the jet impact pressure in static measurements

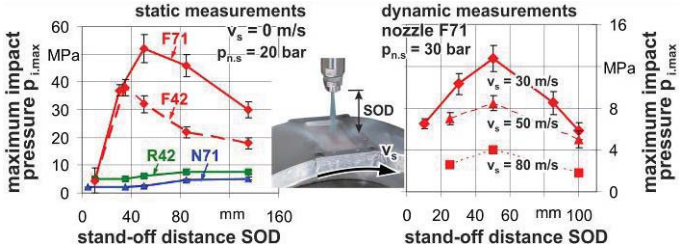

Figure 6. Maximum jet impact pressure in static (left) and dynamic measurements (right)

4 Grinding experiments

The efficiency of cleaning nozzles was investigated in face grinding of superalloy Inconel 718 in the 'up grinding mode' utilizing a vitrified bonded wheel A60H16 (b_s = 20 mm). A 5% emulsion was used as cooling lubricant and cleaning medium. The grinding experiments were carried out with a cutting speed of v_s = 40 m/s and a depth of cut of a_e = 1.2 mm. The specific material removal rate Q_w' was varied via the workpiece feed speed. The length of the workpiece was 100 mm. The grinding forces were measured using a Kistler dynamometer typ 9255b.

In grinding experiments with tool cleaning, the grinding wheel was in-process cleaned by using an additional cleaning nozzle. The cleaning nozzle was positioned in the upper area of the grinding wheel, perpendicular to the circumferential wheel surface. The cleaning jet causes no damages of the wheel bond, since the strength of alumina (compressive strength app. 2,500 MPa, flexural strength app. 350 MPa) is higher than the mechanical stress induced by jet impact (see Fig. 6).

4.1 Measurement of wheel clogging

An optical measurement system 'GrindingVision' was developed to quantify wheel clogging and thus to evaluate the cleaning effect of nozzles in grinding processes (Fig. 7). The measurement system comprises a high-resolution CCD camera with a macro lens and an adaptive illumination system with high-power LEDs. The macro images of the tool surface are analyzed by specially developed software. This software recognizes welded clogging and chip nests by their light reflection and calculates the clogged tool surface area in percent. Following each grinding experiment, clogging at 10 points on the circumferential surface of the grinding wheel was measured and an average of the wheel clogging degree L_s was calculated. For verification, an analysis of the clogging was carried out using a portable light microscope.

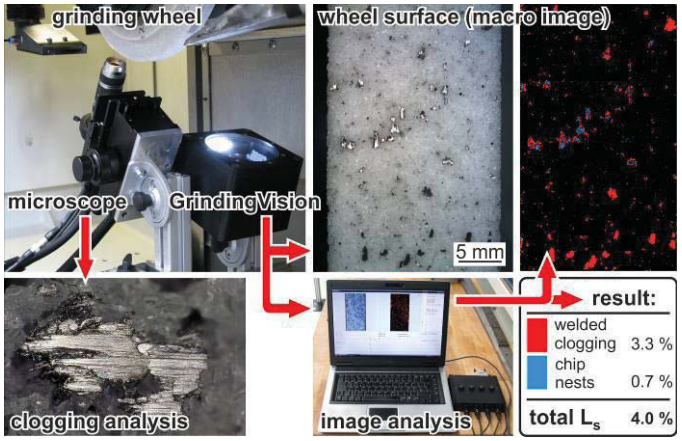

Figure 7. Measurement of wheel clogging

4.2 Investigation of tool cleaning

In grinding experiments without tool cleaning, a continuous increase of wheel clogging L_s from 2.5% up to 4.0% was detected with increased specific material removal rate Q_w' (Fig. 8). The grinding wheel was mainly loaded by welded clogging with a size up to 2 mm. Some small chip nests were observed in tool pores.

By using the cleaning nozzle F71 (SOD = 50 mm, $p_{n.s}$ = 20 bar), a significant reduction of wheel clogging was achieved in grinding experiments with in-process tool cleaning (Fig. 8). Even with high removal rates Q_w' up to 60 mm^3/(mm·s), the wheel clogging degree L_s remained below 1%. Due to the tool cleaning, a high cutting ability the grinding wheel was ensured. In comparison to the grinding without tool cleaning, this led to a decrease in grinding forces from 20% up to 30% and to a reduction in radial wheel wear from 10% up to 20%.

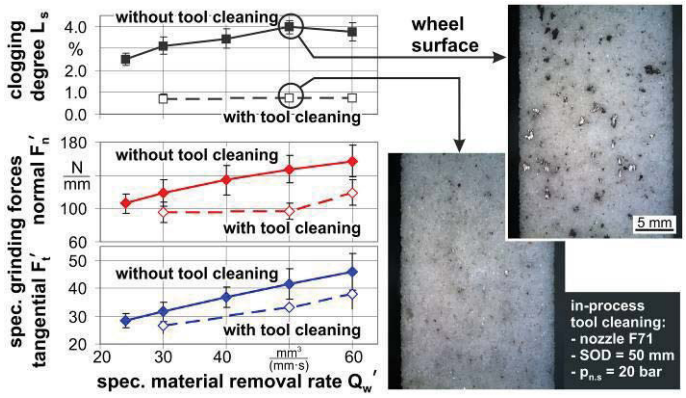

Figure 8. Wheel clogging degree and grinding forces in grinding experiments with/without tool cleaning

The cleaning effect of nozzles F42, F71, N71 and R42 was compared in grinding experiments with a specific material removal rate Q_w' = 50 mm^3/(mm·s), a stand-off distance SOD = 50 mm and a static pressure in the nozzle $p_{n.s}$ = 20 bar. In comparison to the flat fan nozzle F71, the rotor nozzle R42 and the needle nozzle N71 achieve a lower cleaning performance. The

clogging degree increased by 33% (L_s = 1.2%) for nozzle R42 and by 56% (L_s = 1.8%) for nozzle N71 (Fig. 9). The lower cleaning effect of the needle and rotor nozzle leads to around 18% higher grinding forces compared to the grinding with nozzle F71. A reduction of the orifice area from 7.1 to 4.2 mm^2 in flat fan nozzles (F71 and F42) causes a slight increase of wheel clogging (L_s = 0.9%) and grinding forces by around 8%.

In grinding experiments with the nozzle F71 ($p_{n.s}$ = 20 bar), the highest cleaning effect was found at a stand-off distance of *SOD* = 35 – 50 mm (Fig. 10). A reduction as well as an increase of the stand-off distance leads to increased wheel clogging and therefore to around 15% higher grinding forces.

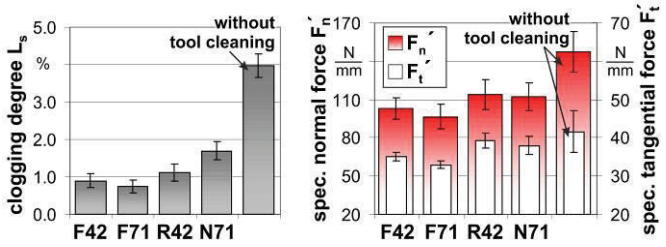

Figure 9. Wheel clogging degree and grinding forces by using different nozzles for tool cleaning

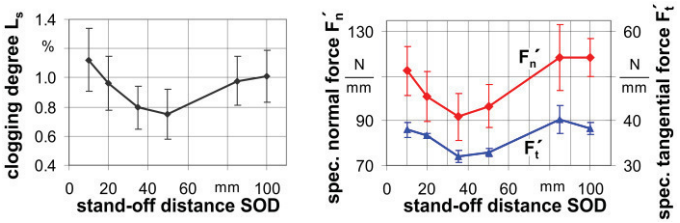

Figure 10. Wheel clogging degree and grinding forces in depending from the nozzle distance (stand-off distance) for nozzle F71

The investigations of the in-process tool cleaning in grinding experiments show the influences of the nozzle design and the nozzle distance on the achievable cleaning effect and the resulting grinding forces. In addition, a correlation between the cleaning effect and the jet impact pressure was found: the achievable cleaning effect is depending on the nozzle design as well as the nozzle position and can be predicted by measurements of the jet impact pressure using pressure sensitive sheets.

5 Conclusions and outlook

In this research work, the in-process tool cleaning by high-speed coolant jet was investigated as a means to prevent wheel clogging in creep feed grinding of Inconel 718. Efficient cleaning parameters were identified by investigating the relationships between the nozzle design, the resulting jet flow properties and the achievable cleaning effect in grinding tests. It was shown that the efficiency of coolant nozzles can be determined by measuring jet velocity and jet impact pressure.

The presented results show the influences of the jet flow properties and the nozzle position on the achievable cleaning effect and the resulting grinding forces. The highest cleaning effect was achieved by using flat fan nozzles. These nozzles are characterized by a higher jet velocity and a higher jet impact pressure compared to the rotor nozzle and the needle nozzles. In alignment with the observed jet impact pressure, the highest cleaning effect and thus the lowest wheel clogging was achieved at a certain nozzle distance from the wheel surface. The effect of stand-off distance is caused by jet turbulences which lead to a high dynamics within the cleaning jet and thus to an increase of its cleaning performance.

An almost clogging-free condition of the grinding wheel can be achieved even at a relatively low pump pressure by optimizing of the cleaning parameters (nozzle configuration, nozzle position). By preventing loading of the grinding wheel, the grinding forces and the tool wear are significantly reduced. This results in higher achievable process performance and workpiece quality.

Based on the findings presented here, a new nozzle concept for low pressure coolant supply with simultaneous tool cleaning is currently being developed for different grinding processes e.g. profile grinding of superalloys, gear grinding, grinding of steel and hard materials with conventional and superabrasive wheels using both, oil and emulsion. This new nozzle concept aims at the increase of the achievable performance and stability of grinding processes as well as at energy savings by adaptively controlled coolant supply for roughing and finishing.

Acknowledgements

The results were derived from the research project IGF 16179 N which was supported by the German Ministry of Economics and Technology (BMWi) via the Industrial Cooperative Research Associations (AiF) and the German Machine Tool Builders‘ Association (VDW – Forschungsinstitut e. V.). The authors thank the cooperating industrial partners for technical support and advice.

References

[1] Lauer-Schmaltz H., König W., 1980, Phenomenon of Wheel Loading Mechanisms in Grinding. CIRP Annals 29/1:201-206.

[2] Khudobin L. V., Unyanin A. N., 2008, Improved Performance of Grinding Wheels in Machining Plastic Steel and Alloy Blanks, Russian Engineering Research 28/12:1190-1195.

[3] Brinksmeier, E., Aurich, J. C., Govekar, E., Heinzel, C., Hoffmeister, H.-W., Klocke, F., Peters, J., Rentsch, R., Stephenson, D. J., Uhlmann, E., Weinert, K., Wittmann, M., 2006, Advances in Modeling and Simulation of Grinding Processes, CIRP Annals 55/2:667-696.

[4] Wegener, K., H.-W. Hoffmeister, H. –W., Karpuschewski, B., Kuster, F., Hahmann, W.-C., Rabiey, M., 2011, Conditioning and monitoring of grinding wheels, CIRP Annals 60(2):757-777.

[5] Webster J., 2008, In Grinding, Coolant Application Matters, Manufacturing Engineering 140/3:19-25.

[6] Webster, J., Brinksmeier, E., Heinzel, C., Wittmann, M., 2002, Assessment of Grinding Fluid Effectiveness in Continuous-Dress Creep Feed Grinding, CIRP Annals 51/1:235-240.

[7] Brinksmeier, E., Heinzel C., Wittmann, M., 1999, Friction, Cooling and Lubrication in Grinding, CIRP Annals 48/2: 581-598.

[8] Jackson, M. J., Khangar, A., Chenc, X., Robinson, G.M., Venkatesh, V.C., Dahotre, N.B., 2007, Laser cleaning and dressing of vitrified grinding wheels, Journal of Materials Processing Technology 185:17–23.

[9] Axinte, D. A., Stepanian, J. P., Kong, M. C., McGourlay, J., 2009, Abrasive waterjet turning - An efficient method to profile and dress grinding wheels, International Journal of Machine Tools & Manufacture 49:351–356.

[10] Cameron, A., Bauer, R., Warkentin, A., 2010, An investigation of the effects of wheel-cleaning parameters in creep-feed grinding, International Journal of Machine Tools & Manufacture 50:126–130

[11] Smith, D. G., Kinslow, R., 1976, Pressure Due to High-velocity Impact of a Water Jet, Experimental Mechanics, 16/1:21-25

[12] Zou, C.-Z., 1985, Investigation on Anatomy of Continuos Waterjet for Updating Jet Performance, Proceedings third US. Waterjet Conference: 132-146

[13] Camus, J. J., 1971, A study of high speed liquid flow in impact and its effect on solid surfaces, PhD thesis, Cambridge University.

[14] Thomas, G. P., Brunton J. H., 1970, Drop impingement erosion of metals, Proceedings of the Royal Society of London A/314: 549–565.

[15] Lesser, M., 1995, Thirty years of liquid impact research: a tutorial review, Wear 186/187:28-34.